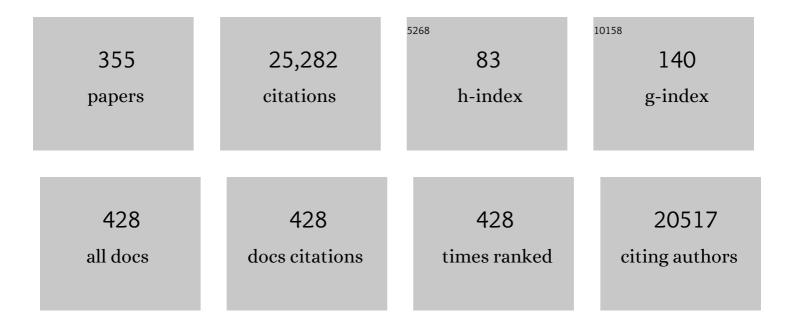
Ayyalusamy Ramamoorthy

List of Publications by Year in descending order

Source: https://exaly.com/author-pdf/8121355/publications.pdf Version: 2024-02-01



#	Article	IF	CITATIONS
1	Molecular Music: A Modern Accompaniment to NMR Pedagogy. Journal of Chemical Education, 2022, 99, 810-818.	2.3	1
2	Conformational Tuning of Amylin by Charged Styrene-Maleic-Acid Copolymers. Journal of Molecular Biology, 2022, 434, 167385.	4.2	6
3	Detergent-free isolation of CYP450-reductase's FMN-binding domain in <i>E. coli</i> lipid-nanodiscs using a charge-free polymer. Chemical Communications, 2022, , .	4.1	8
4	Saponins Form Nonionic Lipid Nanodiscs for Protein Structural Studies by Nuclear Magnetic Resonance Spectroscopy. Journal of Physical Chemistry Letters, 2022, 13, 1705-1712.	4.6	11
5	Measurement of Residual Dipolar Couplings Using Magnetically Aligned and Flipped Nanodiscs. Langmuir, 2022, 38, 244-252.	3.5	7
6	Biophysical processes underlying cross-seeding in amyloid aggregation and implications in amyloid pathology. Biophysical Chemistry, 2021, 269, 106507.	2.8	101
7	Nanodisc reconstitution of flavin mononucleotide binding domain of cytochrome-P450-reductase enables high-resolution NMR probing. Chemical Communications, 2021, 57, 4819-4822.	4.1	5
8	Proteostasis of Islet Amyloid Polypeptide: A Molecular Perspective of Risk Factors and Protective Strategies for Type II Diabetes. Chemical Reviews, 2021, 121, 1845-1893.	47.7	129
9	Amyloid Oligomers: A Joint Experimental/Computational Perspective on Alzheimer's Disease, Parkinson's Disease, Type II Diabetes, and Amyotrophic Lateral Sclerosis. Chemical Reviews, 2021, 121, 2545-2647.	47.7	406
10	Benchmarks of SMA-Copolymer Derivatives and Nanodisc Integrity. Langmuir, 2021, 37, 3113-3121.	3.5	11
11	Solid-state packing dictates the unexpected solubility of aromatic peptides. Cell Reports Physical Science, 2021, 2, 100391.	5.6	10
12	Solid-State NMR Study to Probe the Effects of Divalent Metal Ions (Ca ²⁺ and) Tj ETQq0 0 0 rgBT /C	Overlock 10 3.5) Tf 50 307 To 4
13	Synthesis, Characterization, and Nanodisc Formation of Nonâ€ionic Polymers**. Angewandte Chemie - International Edition, 2021, 60, 16885-16888.	13.8	29
14	Synthesis, Characterization, and Nanodisc Formation of Nonâ€ionic Polymers**. Angewandte Chemie, 2021, 133, 17022-17025.	2.0	5
15	Degradation of Alzheimer's Amyloid-β by a Catalytically Inactive Insulin-Degrading Enzyme. Journal of Molecular Biology, 2021, 433, 166993.	4.2	27
16	Investigation of the effects of two major secretory granules components, insulin and zinc, on human-IAPP amyloid aggregation and membrane damage. Chemistry and Physics of Lipids, 2021, 237, 105083.	3.2	24
17	Lipids on the pathomechanisms of amyloid diseases. Chemistry and Physics of Lipids, 2021, 239, 105122.	3.2	0
18	Aggregation and the Intrinsic Structural Disorder of Dipeptide Repeat Peptides of C9orf72-Related Amyotrophic Lateral Sclerosis and Frontotemporal Dementia Characterized by NMR. Journal of Physical Chemistry B, 2021, 125, 12446-12456.	2.6	2

#	Article	IF	CITATIONS
19	Structural Interaction of Apolipoprotein A-I Mimetic Peptide with Amyloid-Î ² Generates Toxic Hetero-oligomers. Journal of Molecular Biology, 2020, 432, 1020-1034.	4.2	25
20	Lipid-Chaperone Hypothesis: A Common Molecular Mechanism of Membrane Disruption by Intrinsically Disordered Proteins. ACS Chemical Neuroscience, 2020, 11, 4336-4350.	3.5	101
21	Natural-abundance ¹⁷ O NMR spectroscopy of magnetically aligned lipid nanodiscs. Chemical Communications, 2020, 56, 9998-10001.	4.1	10
22	Small molecule induced toxic human-IAPP species characterized by NMR. Chemical Communications, 2020, 56, 13129-13132.	4.1	21
23	High-Throughput Screening at the Membrane Interface Reveals Inhibitors of Amyloid-Î ² . Biochemistry, 2020, 59, 2249-2258.	2.5	40
24	Detergent-free extraction, reconstitution and characterization of membrane-anchored cytochrome-b5 in native lipids. Chemical Communications, 2020, 56, 6511-6514.	4.1	26
25	Lipid-nanodiscs formed by paramagnetic metal chelated polymer for fast NMR data acquisition. Biochimica Et Biophysica Acta - Biomembranes, 2020, 1862, 183332.	2.6	9
26	High-Speed Atomic Force Microscopy Reveals the Structural Dynamics of the Amyloid-Î ² and Amylin Aggregation Pathways. International Journal of Molecular Sciences, 2020, 21, 4287.	4.1	27
27	High-resolution proton-detected MAS experiments on self-assembled diphenylalanine nanotubes enabled by fast MAS and high magnetic field. Journal of Magnetic Resonance, 2020, 313, 106717.	2.1	11
28	Symmetry-breaking transitions in the early steps of protein self-assembly. European Biophysics Journal, 2020, 49, 175-191.	2.2	28
29	Amylin and beta amyloid proteins interact to form amorphous heterocomplexes with enhanced toxicity in neuronal cells. Scientific Reports, 2020, 10, 10356.	3.3	44
30	Magnetic Alignment of Polymer Nanodiscs Probed by Solid-State NMR Spectroscopy. Langmuir, 2020, 36, 1258-1265.	3.5	21
31	Unusual Two‧tep Assembly of a Minimalistic Dipeptideâ€Based Functional Hypergelator. Advanced Materials, 2020, 32, e1906043.	21.0	73
32	Expression, purification, and functional reconstitution of 19F-labeled cytochrome b5 in peptide nanodiscs for NMR studies. Biochimica Et Biophysica Acta - Biomembranes, 2020, 1862, 183194.	2.6	13
33	High-resolution probing of early events in amyloid-β aggregation related to Alzheimer's disease. Chemical Communications, 2020, 56, 4627-4639.	4.1	71
34	Diverse Structural Conversion and Aggregation Pathways of Alzheimer's Amyloid-β (1–40). ACS Nano, 2019, 13, 8766-8783.	14.6	33
35	Magnetic Alignment of Polymer Macroâ€Nanodiscs Enables Residualâ€Dipolarâ€Couplingâ€Based Highâ€Resolution Structural Studies by NMR Spectroscopy. Angewandte Chemie, 2019, 131, 15067-15070.	2.0	7
36	Use of paramagnetic systems to speed-up NMR data acquisition and for structural and dynamic studies. Solid State Nuclear Magnetic Resonance, 2019, 102, 36-46.	2.3	20

#	Article	IF	CITATIONS
37	Magnetic Alignment of Polymer Macroâ€Nanodiscs Enables Residualâ€Dipolarâ€Couplingâ€Based Highâ€Resolution Structural Studies by NMR Spectroscopy. Angewandte Chemie - International Edition, 2019, 58, 14925-14928.	13.8	27
38	Exploiting heterogeneous time scale of dynamics to enhance 2D HETCOR solid-state NMR sensitivity. Journal of Magnetic Resonance, 2019, 309, 106615.	2.1	15
39	Berichtigung: Bioinspired, Sizeâ€Tunable Selfâ€Assembly of Polymer—Lipid Bilayer Nanodiscs. Angewandte Chemie, 2019, 131, 13318-13318.	2.0	2
40	Metal helated Polymer Nanodiscs for NMR Studies. Angewandte Chemie, 2019, 131, 17406-17410.	2.0	2
41	Metalâ€Chelated Polymer Nanodiscs for NMR Studies. Angewandte Chemie - International Edition, 2019, 58, 17246-17250.	13.8	16
42	Berichtigung: Formation of pHâ€Resistant Monodispersed Polymer—Lipid Bilayer Nanodiscs. Angewandte Chemie, 2019, 131, 13319-13319.	2.0	2
43	Polymer nanodiscs: Advantages and limitations. Chemistry and Physics of Lipids, 2019, 219, 45-49.	3.2	77
44	Hydrophobic Functionalization of Polyacrylic Acid as a Versatile Platform for the Development of Polymer Lipid Nanodisks. Small, 2019, 15, e1804813.	10.0	43
45	NMR-Based Metabolomic Profiling of Urine: Evaluation for Application in Prostate Cancer Detection. Natural Product Communications, 2019, 14, 1934578X1984997.	0.5	7
46	Self-Assembly of Polymer-Encased Lipid Nanodiscs and Membrane Protein Reconstitution. Journal of Physical Chemistry B, 2019, 123, 4562-4570.	2.6	22
47	Probing membrane enhanced protein–protein interactions in a minimal redox complex of cytochrome-P450 and P450-reductase. Chemical Communications, 2019, 55, 5777-5780.	4.1	15
48	Probing transient non-native states in amyloid beta fiber elongation by NMR. Chemical Communications, 2019, 55, 4483-4486.	4.1	46
49	A cationic polymethacrylate-copolymer acts as an agonist for β-amyloid and an antagonist for amylin fibrillation. Chemical Science, 2019, 10, 3976-3986.	7.4	52
50	Probing protein–protein and protein–substrate interactions in the dynamic membrane-associated ternary complex of cytochromes P450, <i>b</i> ₅ , and reductase. Chemical Communications, 2019, 55, 13422-13425.	4.1	17
51	Proton-detected 3D 1H anisotropic/14N/1H isotropic chemical shifts correlation NMR under fast magic angle spinning on solid samples withoutÂisotopic enrichment. Solid State Nuclear Magnetic Resonance, 2019, 97, 40-45.	2.3	9
52	Zinc boosts EGCG's hIAPP amyloid Inhibition both in solution and membrane. Biochimica Et Biophysica Acta - Proteins and Proteomics, 2019, 1867, 529-536.	2.3	32
53	Semenâ€derived amyloidogenic peptides—Key players of HIV infection. Protein Science, 2018, 27, 1151-1165.	7.6	15
54	Cytochromeâ€P450â€Induced Ordering of Microsomal Membranes Modulates Affinity for Drugs. Angewandte Chemie, 2018, 130, 3449-3453.	2.0	5

#	Article	IF	CITATIONS
55	Cytochromeâ€P450â€Induced Ordering of Microsomal Membranes Modulates Affinity for Drugs. Angewandte Chemie - International Edition, 2018, 57, 3391-3395.	13.8	44
56	Real-time monitoring of the aggregation of Alzheimer's amyloid-β <i>via</i> ¹ H magic angle spinning NMR spectroscopy. Chemical Communications, 2018, 54, 2000-2003.	4.1	28
57	Unusual multiscale mechanics of biomimetic nanoparticle hydrogels. Nature Communications, 2018, 9, 181.	12.8	28
58	A Minimal Functional Complex of Cytochrome P450 and FBD of Cytochrome P450 Reductase in Nanodiscs. Angewandte Chemie - International Edition, 2018, 57, 8458-8462.	13.8	36
59	Impact of membrane curvature on amyloid aggregation. Biochimica Et Biophysica Acta - Biomembranes, 2018, 1860, 1741-1764.	2.6	88
60	Real-Time Monitoring of Lipid Exchange via Fusion of Peptide Based Lipid-Nanodiscs. Chemistry of Materials, 2018, 30, 3204-3207.	6.7	23
61	Engineering <scp>l</scp> -asparaginase for spontaneous formation of calcium phosphate bioinspired microreactors. Physical Chemistry Chemical Physics, 2018, 20, 12719-12726.	2.8	9
62	hIAPP forms toxic oligomers in plasma. Chemical Communications, 2018, 54, 5426-5429.	4.1	28
63	A blend of two resveratrol derivatives abolishes hIAPP amyloid growth and membrane damage. Biochimica Et Biophysica Acta - Biomembranes, 2018, 1860, 1793-1802.	2.6	36
64	Dynamic membrane interactions of antibacterial and antifungal biomolecules, and amyloid peptides, revealed by solid-state NMR spectroscopy. Biochimica Et Biophysica Acta - General Subjects, 2018, 1862, 307-323.	2.4	37
65	Formation of pHâ€Resistant Monodispersed Polymer–Lipid Nanodiscs. Angewandte Chemie - International Edition, 2018, 57, 1342-1345.	13.8	106
66	Formation of pHâ€Resistant Monodispersed Polymer–Lipid Nanodiscs. Angewandte Chemie, 2018, 130, 1356-1359.	2.0	7
67	Alzheimer's amyloid-beta intermediates generated using polymer-nanodiscs. Chemical Communications, 2018, 54, 12883-12886.	4.1	69
68	Cytochrome P450 Prefers to be in Liquid-Ordered Domains in the Endoplasmic Reticulum. Biophysical Journal, 2018, 114, 71a.	0.5	0
69	Styrene maleic acid derivates to enhance the applications of bio-inspired polymer based lipid-nanodiscs. European Polymer Journal, 2018, 108, 597-602.	5.4	22
70	Nanodisc-Forming Scaffold Protein Promoted Retardation of Amyloid-Beta Aggregation. Journal of Molecular Biology, 2018, 430, 4230-4244.	4.2	49
71	The Influence of Chemical Modification on Linker Rotational Dynamics in Metal–Organic Frameworks. Angewandte Chemie - International Edition, 2018, 57, 8678-8681.	13.8	33
72	The Influence of Chemical Modification on Linker Rotational Dynamics in Metal–Organic Frameworks. Angewandte Chemie, 2018, 130, 8814-8817.	2.0	11

#	Article	IF	CITATIONS
73	Lipid-exchange in nanodiscs discloses membrane boundaries of cytochrome-P450 reductase. Chemical Communications, 2018, 54, 6336-6339.	4.1	15
74	High-Resolution Proton NMR Spectroscopy of Polymers and Biological Solids. , 2018, , 521-536.		2
75	Effect of polymer charge on functional reconstitution of membrane proteins in polymer nanodiscs. Chemical Communications, 2018, 54, 9615-9618.	4.1	52
76	Picturing the Membraneâ€assisted Choreography of Cytochrome P450 with Lipid Nanodiscs. ChemPhysChem, 2018, 19, 2603-2613.	2.1	28
77	Substrate mediated redox partner selectivity of cytochrome P450. Chemical Communications, 2018, 54, 5780-5783.	4.1	11
78	Preparation of Stable Amyloid-Î ² Oligomers Without Perturbative Methods. Methods in Molecular Biology, 2018, 1777, 331-338.	0.9	6
79	A Minimal Functional Complex of Cytochrome P450 and FBD of Cytochrome P450 Reductase in Nanodiscs. Angewandte Chemie, 2018, 130, 8594-8598.	2.0	6
80	Reduced Lipid Bilayer Thickness Regulates the Aggregation and Cytotoxicity of Amyloid-β. Journal of Biological Chemistry, 2017, 292, 4638-4650.	3.4	145
81	Conformations and Intermolecular Interactions in Cellulose/Silk Fibroin Blend Films: A Solid-State NMR Perspective. Journal of Physical Chemistry B, 2017, 121, 6108-6116.	2.6	47
82	3D Double-Quantum/Double-Quantum Exchange Spectroscopy of Protons under 100 kHz Magic Angle Spinning. Journal of Physical Chemistry B, 2017, 121, 5944-5952.	2.6	16
83	Model membrane size-dependent amyloidogenesis of Alzheimer's amyloid-β peptides. Physical Chemistry Chemical Physics, 2017, 19, 16257-16266.	2.8	42
84	Proton-Based Ultrafast Magic Angle Spinning Solid-State NMR Spectroscopy. Accounts of Chemical Research, 2017, 50, 1105-1113.	15.6	111
85	Structural and Mechanistic Insights into Development of Chemical Tools to Control Individual and Interâ€Related Pathological Features in Alzheimer's Disease. Chemistry - A European Journal, 2017, 23, 2706-2715.	3.3	25
86	Electrostatic Constraints Assessed by ¹ H MAS NMR Illuminate Differences in Crystalline Polymorphs. Journal of Physical Chemistry Letters, 2017, 8, 4253-4257.	4.6	15
87	pH Tunable and Divalent Metal Ion Tolerant Polymer Lipid Nanodiscs. Langmuir, 2017, 33, 10655-10662.	3.5	75
88	Kinetic and Structural Characterization of the Effects of Membrane on the Complex of Cytochrome b 5 and Cytochrome c. Scientific Reports, 2017, 7, 7793.	3.3	15
89	Bioinspired, Sizeâ€Tunable Selfâ€Assembly of Polymer–Lipid Bilayer Nanodiscs. Angewandte Chemie, 2017, 129, 11624-11628.	2.0	25
90	Bioinspired, Sizeâ€Tunable Selfâ€Assembly of Polymer–Lipid Bilayer Nanodiscs. Angewandte Chemie - International Edition, 2017, 56, 11466-11470.	13.8	120

#	Article	IF	CITATIONS
91	Growth-incompetent monomers of human calcitonin lead to a noncanonical direct relationship between peptide concentration and aggregation lag time. Journal of Biological Chemistry, 2017, 292, 14963-14976.	3.4	16
92	Role of Anomalous Water Constraints in the Efficacy of Pharmaceuticals Probed by 1 H Solidâ€State NMR. ChemistrySelect, 2017, 2, 6797-6800.	1.5	12
93	Spontaneous Lipid Nanodisc Fomation by Amphiphilic Polymethacrylate Copolymers. Journal of the American Chemical Society, 2017, 139, 18657-18663.	13.7	101
94	Membrane environment drives cytochrome P450's spin transition and its interaction with cytochrome <i>b</i> ₅ . Chemical Communications, 2017, 53, 12798-12801.	4.1	40
95	Solid-State NMR Spectroscopy: The Magic Wand to View Bone at Nanoscopic Resolution. Annual Reports on NMR Spectroscopy, 2017, 92, 365-413.	1.5	17
96	Minor Structural Variations of Small Molecules Tune Regulatory Activities toward Pathological Factors in Alzheimer's Disease. ChemMedChem, 2017, 12, 1828-1838.	3.2	13
97	Transmembrane Interactions of Full-length Mammalian Bitopic Cytochrome-P450-Cytochrome-b5 Complex in Lipid Bilayers Revealed by Sensitivity-Enhanced Dynamic Nuclear Polarization Solid-state NMR Spectroscopy. Scientific Reports, 2017, 7, 4116.	3.3	32
98	Accelerated molecular dynamics simulation analysis of MSI-594 in a lipid bilayer. Physical Chemistry Chemical Physics, 2017, 19, 19289-19299.	2.8	46
99	Structural Biology of Calcitonin: From Aqueous Therapeutic Properties to Amyloid Aggregation. Israel Journal of Chemistry, 2017, 57, 634-650.	2.3	15
100	An Iridium(III) Complex as a Photoactivatable Tool for Oxidation of Amyloidogenic Peptides with Subsequent Modulation of Peptide Aggregation. Chemistry - A European Journal, 2017, 23, 1645-1653.	3.3	33
101	Stabilization and structural analysis of a membrane-associated hIAPP aggregation intermediate. ELife, 2017, 6, .	6.0	61
102	Multi-target-directed phenol–triazole ligands as therapeutic agents for Alzheimer's disease. Chemical Science, 2017, 8, 5636-5643.	7.4	79
103	The catalytic function of cytochrome P450 is entwined with its membrane-bound nature. F1000Research, 2017, 6, 662.	1.6	51
104	High-Resolution Proton NMR Spectroscopy of Polymers and Biological Solids. , 2017, , 1-16.		0
105	Inhibition of IAPP Aggregation and Toxicity by Natural Products and Derivatives. Journal of Diabetes Research, 2016, 2016, 1-12.	2.3	109
106	The Role of Cholesterol in Driving IAPP-Membrane Interactions. Biophysical Journal, 2016, 111, 140-151.	0.5	74
107	Enhancing NMR Sensitivity of Naturalâ€Abundance Lowâ€Î³ Nuclei by Ultrafast Magicâ€Angleâ€5pinning Solidâ€State NMR Spectroscopy. ChemPhysChem, 2016, 17, 2962-2966.	2.1	30
108	Constant-time 2D and 3D through-bond correlation NMR spectroscopy of solids under 60 kHz MAS. Journal of Chemical Physics, 2016, 144, 034202.	3.0	11

#	Article	IF	CITATIONS
109	Proton-detected 3D 15N/1H/1H isotropic/anisotropic/isotropic chemical shift correlation solid-state NMR at 70kHz MAS. Solid State Nuclear Magnetic Resonance, 2016, 76-77, 1-6.	2.3	16
110	Multifunctional quinoline-triazole derivatives as potential modulators of amyloid-β peptide aggregation. Journal of Inorganic Biochemistry, 2016, 158, 131-138.	3.5	25
111	Hybridizing cross-polarization with NOE or refocused-INEPT enhances the sensitivity of MAS NMR spectroscopy. Journal of Magnetic Resonance, 2016, 266, 59-66.	2.1	33
112	Importance of the Dimethylamino Functionality on a Multifunctional Framework for Regulating Metals, Amyloid-β, and Oxidative Stress in Alzheimer's Disease. Inorganic Chemistry, 2016, 55, 5000-5013.	4.0	19
113	Spontaneous structural transition and crystal formation in minimal supramolecular polymer model. Science Advances, 2016, 2, e1500827.	10.3	62
114	Mode of Action of a Designed Antimicrobial Peptide: High Potency against Cryptococcus neoformans. Biophysical Journal, 2016, 111, 1724-1737.	0.5	37
115	Selective detection and complete identification of triglycerides in cortical bone by high-resolution ¹ H MAS NMR spectroscopy. Physical Chemistry Chemical Physics, 2016, 18, 18687-18691.	2.8	22
116	Reconstitution of the Cyt <i>b</i> ₅ –CytP450 Complex in Nanodiscs for Structural Studies using NMR Spectroscopy. Angewandte Chemie, 2016, 128, 4573-4575.	2.0	13
117	Biophysical insights into the membrane interaction of the core amyloid-forming Aβ ₄₀ fragment K16–K28 and its role in the pathogenesis of Alzheimer's disease. Physical Chemistry Chemical Physics, 2016, 18, 16890-16901.	2.8	16
118	Reconstitution of the Cytb5-CytP450 Complex in Nanodiscs for Structural Studies using NMR Spectroscopy. Angewandte Chemie - International Edition, 2016, 55, 4497-4499.	13.8	80
119	Effects of hydroxyl group variations on a flavonoid backbone toward modulation of metal-free and metal-induced amyloid-l ² aggregation. Inorganic Chemistry Frontiers, 2016, 3, 381-392.	6.0	28
120	Amyloid-Î ² adopts a conserved, partially folded structure upon binding to zwitterionic lipid bilayers prior to amyloid formation. Chemical Communications, 2016, 52, 882-885.	4.1	66
121	Influence of a curcumin derivative on hIAPP aggregation in the absence and presence of lipid membranes. Chemical Communications, 2016, 52, 942-945.	4.1	63
122	Proton chemical shift tensors determined by 3D ultrafast MAS double-quantum NMR spectroscopy. Journal of Chemical Physics, 2015, 143, 144201.	3.0	28
123	Reactivity of Metal-Free and Metal-Associated Amyloid-Î ² with Glycosylated Polyphenols and Their Esterified Derivatives. Scientific Reports, 2015, 5, 17842.	3.3	44
124	Proton-detected 3D 1H/13C/1H correlation experiment for structural analysis in rigid solids under ultrafast-MAS above 60 kHz. Journal of Chemical Physics, 2015, 143, 164201.	3.0	16
125	Effects of Membrane Mimetics on Cytochrome P450-Cytochrome b5 Interactions Characterized by NMR Spectroscopy. Journal of Biological Chemistry, 2015, 290, 12705-12718.	3.4	30
126	Insights into the Role of Substrates on the Interaction between Cytochrome b5 and Cytochrome P450 2B4 by NMR. Scientific Reports, 2015, 5, 8392.	3.3	24

#	Article	IF	CITATIONS
127	Probing the Sources of the Apparent Irreproducibility of Amyloid Formation: Drastic Changes in Kinetics and a Switch in Mechanism Due to Micellelike Oligomer Formation at Critical Concentrations of IAPP. Journal of Physical Chemistry B, 2015, 119, 2886-2896.	2.6	85
128	Phase cycling schemes for finite-pulse-RFDR MAS solid state NMR experiments. Journal of Magnetic Resonance, 2015, 252, 55-66.	2.1	43
129	Temperature-Resistant Bicelles for Structural Studies by Solid-State NMR Spectroscopy. Langmuir, 2015, 31, 1496-1504.	3.5	16
130	Investigating Albendazole Desmotropes by Solid-State NMR Spectroscopy. Molecular Pharmaceutics, 2015, 12, 731-741.	4.6	42
131	Membrane interaction of antimicrobial peptides using E. coli lipid extract as model bacterial cell membranes and SFG spectroscopy. Chemistry and Physics of Lipids, 2015, 187, 20-33.	3.2	28
132	Bioanalytical methods for metabolomic profiling: Detection of head and neck cancer, including oral cancer. Chinese Chemical Letters, 2015, 26, 407-415.	9.0	24
133	Antimicrobial Peptides: Insights into Membrane Permeabilization, Lipopolysaccharide Fragmentation and Application in Plant Disease Control. Scientific Reports, 2015, 5, 11951.	3.3	70
134	Proton-Detected Solid-State NMR Spectroscopy of Bone with Ultrafast Magic Angle Spinning. Scientific Reports, 2015, 5, 11991.	3.3	81
135	A Novel High-Resolution and Sensitivity-Enhanced Three-Dimensional Solid-State NMR Experiment Under Ultrafast Magic Angle Spinning Conditions. Scientific Reports, 2015, 5, 11810.	3.3	44
136	High-resolution NMR characterization of low abundance oligomers of amyloid-β without purification. Scientific Reports, 2015, 5, 11811.	3.3	101
137	Self-Assembly of a Nine-Residue Amyloid-Forming Peptide Fragment of SARS Corona Virus E-Protein: Mechanism of Self Aggregation and Amyloid-Inhibition of hIAPP. Biochemistry, 2015, 54, 2249-2261.	2.5	50
138	Detergent-Type Membrane Fragmentation by MSI-78, MSI-367, MSI-594, and MSI-843 Antimicrobial Peptides and Inhibition by Cholesterol: A Solid-State Nuclear Magnetic Resonance Study. Biochemistry, 2015, 54, 1897-1907.	2.5	55
139	1020 MHz single-channel proton fast magic angle spinning solid-state NMR spectroscopy. Journal of Magnetic Resonance, 2015, 261, 1-5.	2.1	38
140	Dynamics-based selective 2D 1H/1H chemical shift correlation spectroscopy under ultrafast MAS conditions. Journal of Chemical Physics, 2015, 142, 204201.	3.0	16
141	Selective excitation enables assignment of proton resonances and 1H-1H distance measurement in ultrafast magic angle spinning solid state NMR spectroscopy. Journal of Chemical Physics, 2015, 143, 034201.	3.0	21
142	A Redox-Active, Compact Molecule for Cross-Linking Amyloidogenic Peptides into Nontoxic, Off-Pathway Aggregates: In Vitro and In Vivo Efficacy and Molecular Mechanisms. Journal of the American Chemical Society, 2015, 137, 14785-14797.	13.7	65
143	Kinetic and Structural Characterization of the Interaction between the FMN Binding Domain of Cytochrome P450 Reductase and Cytochrome c. Journal of Biological Chemistry, 2015, 290, 4843-4855.	3.4	20
144	A cross-polarization based rotating-frame separated-local-field NMR experiment under ultrafast MAS conditions. Journal of Magnetic Resonance, 2015, 250, 37-44.	2.1	32

#	Article	IF	CITATIONS
145	Composite-180° pulse-based symmetry sequences to recouple proton chemical shift anisotropy tensors under ultrafast MAS solid-state NMR spectroscopy. Journal of Magnetic Resonance, 2015, 250, 45-54.	2.1	53
146	Membrane disruptive antimicrobial activities of human β-defensin-3 analogs. European Journal of Medicinal Chemistry, 2015, 91, 91-99.	5.5	44
147	Cellular solid-state NMR investigation of a membrane protein using dynamic nuclear polarization. Biochimica Et Biophysica Acta - Biomembranes, 2015, 1848, 342-349.	2.6	72
148	Nisin ZP, a Bacteriocin and Food Preservative, Inhibits Head and Neck Cancer Tumorigenesis and Prolongs Survival. PLoS ONE, 2015, 10, e0131008.	2.5	143
149	Modulation of raft domains in a lipid bilayer by boundary-active curcumin. Chemical Communications, 2014, 50, 3427.	4.1	44
150	1H, 13C and 15N resonance assignments for the full-length mammalian cytochrome b5 in a membrane environment. Biomolecular NMR Assignments, 2014, 8, 409-413.	0.8	6
151	Potent Î ³ -secretase inhibitors/modulators interact with amyloid-Î ² fibrils but do not inhibit fibrillation: A high-resolution NMR study. Biochemical and Biophysical Research Communications, 2014, 447, 590-595.	2.1	17
152	Acceleration of natural-abundance solid-state MAS NMR measurements on bone by paramagnetic relaxation from gadolinium-DTPA. Journal of Magnetic Resonance, 2014, 244, 90-97.	2.1	21
153	A small molecule that displays marked reactivity toward copper– versus zinc–amyloid-β implicated in Alzheimer's disease. Chemical Communications, 2014, 50, 5301-5303.	4.1	49
154	Differences between amyloid-β aggregation in solution and on the membrane: insights into elucidation of the mechanistic details of Alzheimer's disease. Chemical Society Reviews, 2014, 43, 6692-6700.	38.1	341
155	Rational Design of a Structural Framework with Potential Use to Develop Chemical Reagents That Target and Modulate Multiple Facets of Alzheimer's Disease. Journal of the American Chemical Society, 2014, 136, 299-310.	13.7	166
156	Interaction and reactivity of synthetic aminoisoflavones with metal-free and metal-associated amyloid-l². Chemical Science, 2014, 5, 4851-4862.	7.4	50
157	Non-selective ion channel activity of polymorphic human islet amyloid polypeptide (amylin) double channels. Physical Chemistry Chemical Physics, 2014, 16, 2368-2377.	2.8	36
158	Insights into Atomic-Level Interaction between Mefenamic Acid and Eudragit EPO in a Supersaturated Solution by High-Resolution Magic-Angle Spinning NMR Spectroscopy. Molecular Pharmaceutics, 2014, 11, 351-357.	4.6	48
159	Finite-pulse radio frequency driven recoupling with phase cycling for 2D 1H/1H correlation at ultrafast MAS frequencies. Journal of Magnetic Resonance, 2014, 243, 25-32.	2.1	53
160	Bicelles Exhibiting Magnetic Alignment for a Broader Range of Temperatures: A Solid-State NMR Study. Langmuir, 2014, 30, 1622-1629.	3.5	22
161	In Search of Aggregation Pathways of IAPP and Other Amyloidogenic Proteins: Finding Answers through NMR Spectroscopy. Journal of Physical Chemistry Letters, 2014, 5, 1864-1870.	4.6	77
162	Proton-detected 2D radio frequency driven recoupling solid-state NMR studies on micelle-associated cytochrome-b5. Journal of Magnetic Resonance, 2014, 242, 169-179.	2.1	20

#	Article	IF	CITATIONS
163	3D 15N/15N/1H chemical shift correlation experiment utilizing an RFDR-based 1H/1H mixing period at 100kHz MAS. Journal of Magnetic Resonance, 2014, 244, 1-5.	2.1	56
164	Probing the Transmembrane Structure and Dynamics of Microsomal NADPH-cytochrome P450 oxidoreductase by Solid-State NMR. Biophysical Journal, 2014, 106, 2126-2133.	0.5	38
165	Performance of RINEPT is amplified by dipolar couplings under ultrafast MAS conditions. Journal of Magnetic Resonance, 2014, 243, 85-92.	2.1	17
166	Comparative Analysis of Full-Length Cytochromes P450 in Complexes with Cytochrome B5 in Membrane. Biophysical Journal, 2014, 106, 266a.	0.5	0
167	HR-MAS NMR Tissue Metabolomic Signatures Cross-validated by Mass Spectrometry Distinguish Bladder Cancer from Benign Disease. Journal of Proteome Research, 2013, 12, 3519-3528.	3.7	54
168	On the Role of NMR Spectroscopy for Characterization of Antimicrobial Peptides. Methods in Molecular Biology, 2013, 1063, 159-180.	0.9	34
169	Physiologically-Relevant Modes of Membrane Interactions by the Human Antimicrobial Peptide, LL-37, Revealed by SFG Experiments. Scientific Reports, 2013, 3, 1854.	3.3	51
170	Dynamic Interaction Between Membrane-Bound Full-Length Cytochrome P450 and Cytochrome b5 Observed by Solid-State NMR Spectroscopy. Scientific Reports, 2013, 3, 2538.	3.3	55
171	Insights into Novel Supramolecular Complexes of Two Solid Forms of Norfloxacin and β-Cyclodextrin. Journal of Pharmaceutical Sciences, 2013, 102, 3717-3724.	3.3	30
172	Probing the Transmembrane Structure and Topology of Microsomal Cytochrome-P450 by Solid-State NMR on Temperature-Resistant Bicelles. Scientific Reports, 2013, 3, 2556.	3.3	53
173	Gangliosides Mediate a Two-Step Mechanism of Membrane Disruption byÂBeta-Amyloid: Initial Pore Formation Followed by Membrane Fragmentation. Biophysical Journal, 2013, 104, 217a.	0.5	2
174	Shortening spin–lattice relaxation using a copper-chelated lipid at low-temperatures – A magic angle spinning solid-state NMR study on a membrane-bound protein. Journal of Magnetic Resonance, 2013, 237, 175-181.	2.1	13
175	Cytochrome-P450–Cytochrome- <i>b</i> ₅ Interaction in a Membrane Environment Changes ¹⁵ N Chemical Shift Anisotropy Tensors. Journal of Physical Chemistry B, 2013, 117, 13851-13860.	2.6	15
176	A Model of the Membrane-bound Cytochrome b5-Cytochrome P450 Complex from NMR and Mutagenesis Data. Journal of Biological Chemistry, 2013, 288, 22080-22095.	3.4	105
177	Membrane disordering is not sufficient for membrane permeabilization by islet amyloid polypeptide: studies of IAPP(20–29) fragments. Physical Chemistry Chemical Physics, 2013, 15, 8908.	2.8	60
178	Structural Characterization and Inhibition of Toxic Amyloid-β Oligomeric Intermediates. Biophysical Journal, 2013, 105, 287-288.	0.5	36
179	Zinc stabilization of prefibrillar oligomers of human islet amyloid polypeptide. Chemical Communications, 2013, 49, 3339.	4.1	72
180	Insights into protein misfolding and amyloidogenesis. Physical Chemistry Chemical Physics, 2013, 15, 8867.	2.8	11

#	Article	IF	CITATIONS
181	Quantum Chemical Calculations of Amide-15N Chemical Shift Anisotropy Tensors for a Membrane-Bound Cytochrome-b5. Journal of Physical Chemistry B, 2013, 117, 859-867.	2.6	9
182	Crystallinity and compositional changes in carbonated apatites: Evidence from 31P solid-state NMR, Raman, and AFM analysis. Journal of Solid State Chemistry, 2013, 206, 192-198.	2.9	74
183	Resolution of Oligomeric Species during the Aggregation of Al̂² _{1–40} Using ¹⁹ F NMR. Biochemistry, 2013, 52, 1903-1912.	2.5	97
184	Insights into antiamyloidogenic properties of the green tea extract (â^')-epigallocatechin-3-gallate toward metal-associated amyloid-β species. Proceedings of the National Academy of Sciences of the United States of America, 2013, 110, 3743-3748.	7.1	221
185	Cations as Switches of Amyloid-Mediated Membrane Disruption Mechanisms: Calcium and IAPP. Biophysical Journal, 2013, 104, 173-184.	0.5	103
186	When detergent meets bilayer: Birth and coming of age of lipid bicelles. Progress in Nuclear Magnetic Resonance Spectroscopy, 2013, 69, 1-22.	7.5	106
187	Lipid Composition-Dependent Membrane Fragmentation and Pore-Forming Mechanisms of Membrane Disruption by Pexiganan (MSI-78). Biochemistry, 2013, 52, 3254-3263.	2.5	63
188	2D ¹ H/ ¹ H RFDR and NOESY NMR Experiments on a Membrane-Bound Antimicrobial Peptide Under Magic Angle Spinning. Journal of Physical Chemistry B, 2013, 117, 6693-6700.	2.6	43
189	MetabolD: A graphical user interface package for assignment of 1H NMR spectra of bodyfluids and tissues. Journal of Magnetic Resonance, 2013, 226, 93-99.	2.1	24
190	3P069 Amyloid-like fibrillization and the structure of human calcitonin in the presence of acidic lipids(01C. Protein: Property,Poster). Seibutsu Butsuri, 2013, 53, S223.	0.1	0
191	Bacterial curli protein promotes the conversion of PAP ₂₄₈₋₂₈₆ into the amyloid SEVI: cross-seeding of dissimilar amyloid sequences. PeerJ, 2013, 1, e5.	2.0	73
192	Does Cholesterol Play a Role in the Bacterial Selectivity of Antimicrobial Peptides?. Frontiers in Immunology, 2012, 3, 195.	4.8	97
193	Dual-function triazole–pyridine derivatives as inhibitors of metal-induced amyloid-β aggregation. Metallomics, 2012, 4, 910.	2.4	58
194	Androgen receptor activation results in metabolite signatures of an aggressive prostate cancer phenotype: an NMR-based metabonomics study. Metabolomics, 2012, 8, 1026-1036.	3.0	14
195	Metabolomic Signatures in Guinea Pigs Infected with Epidemic-Associated W-Beijing Strains of Mycobacterium tuberculosis. Journal of Proteome Research, 2012, 11, 4873-4884.	3.7	47
196	Site Specific Interaction of the Polyphenol EGCG with the SEVI Amyloid Precursor Peptide PAP(248–286). Journal of Physical Chemistry B, 2012, 116, 3650-3658.	2.6	83
197	High-Resolution Structural Insights into Bone: A Solid-State NMR Relaxation Study Utilizing Paramagnetic Doping. Journal of Physical Chemistry B, 2012, 116, 11656-11661.	2.6	50
198	NMR Characterization of Monomeric and Oligomeric Conformations of Human Calcitonin and Its Interaction with EGCG. Journal of Molecular Biology, 2012, 416, 108-120.	4.2	66

#	Article	IF	CITATIONS
199	Membrane Disruption and Early Events in the Aggregation of the Diabetes Related Peptide IAPP from a Molecular Perspective. Accounts of Chemical Research, 2012, 45, 454-462.	15.6	322
200	Pseudonegative Thermal Expansion and the State of Water in Graphene Oxide Layered Assemblies. ACS Nano, 2012, 6, 8357-8365.	14.6	136
201	The Magic of Bicelles Lights Up Membrane Protein Structure. Chemical Reviews, 2012, 112, 6054-6074.	47.7	305
202	Alternative Pathways of Human Islet Amyloid Polypeptide Aggregation Distinguished by ¹⁹ F Nuclear Magnetic Resonance-Detected Kinetics of Monomer Consumption. Biochemistry, 2012, 51, 8154-8162.	2.5	118
203	Does cholesterol suppress the antimicrobial peptide induced disruption of lipid raft containing membranes?. Biochimica Et Biophysica Acta - Biomembranes, 2012, 1818, 3019-3024.	2.6	80
204	Delineating metabolic signatures of head and neck squamous cell carcinoma: Phospholipase A2, a potential therapeutic target. International Journal of Biochemistry and Cell Biology, 2012, 44, 1852-1861.	2.8	87
205	Two-Step Mechanism of Membrane Disruption by AÎ ² through Membrane Fragmentation and Pore Formation. Biophysical Journal, 2012, 103, 702-710.	0.5	326
206	Phosphatidylethanolamine Enhances Amyloid Fiber-Dependent Membrane Fragmentation. Biochemistry, 2012, 51, 7676-7684.	2.5	103
207	Determination of ¹⁵ N Chemical Shift Anisotropy from a Membrane-Bound Protein by NMR Spectroscopy. Journal of Physical Chemistry B, 2012, 116, 7181-7189.	2.6	15
208	Side-Chain Dynamics Reveals Transient Association of Aβ _{1–40} Monomers with Amyloid Fibers. Journal of Physical Chemistry B, 2012, 116, 13618-13623.	2.6	26
209	Misfolded proteins in Alzheimer's disease and type II diabetes. Chemical Society Reviews, 2012, 41, 608-621.	38.1	335
210	Coherent averaging in the frequency domain. Journal of Chemical Physics, 2012, 136, 214504.	3.0	5
211	Variable Reference Alignment: An Improved Peak Alignment Protocol for NMR Spectral Data with Large Intersample Variation. Analytical Chemistry, 2012, 84, 5372-5379.	6.5	26
212	Solid-State NMR Spectroscopy Provides Atomic-Level Insights Into the Dehydration of Cartilage. Journal of Physical Chemistry B, 2011, 115, 9948-9954.	2.6	41
213	Role of Cationic Group Structure in Membrane Binding and Disruption by Amphiphilic Copolymers. Journal of Physical Chemistry B, 2011, 115, 366-375.	2.6	151
214	A Proton Spin Diffusion Based Solid-State NMR Approach for Structural Studies on Aligned Samples. Journal of Physical Chemistry B, 2011, 115, 4863-4871.	2.6	10
215	Fast NMR Data Acquisition From Bicelles Containing a Membrane-Associated Peptide at Natural-Abundance. Journal of Physical Chemistry B, 2011, 115, 12448-12455.	2.6	33
216	Membrane Orientation of MSI-78 Measured by Sum Frequency Generation Vibrational Spectroscopy. Langmuir, 2011, 27, 7760-7767.	3.5	78

#	Article	IF	CITATIONS
217	Biphasic Effects of Insulin on Islet Amyloid Polypeptide Membrane Disruption. Biophysical Journal, 2011, 100, 685-692.	0.5	88
218	An Active Photoreceptor Intermediate Revealed by In Situ Photoirradiated Solid-State NMR Spectroscopy. Biophysical Journal, 2011, 101, L50-L52.	0.5	26
219	Magic Angle Spinning NMR-Based Metabolic Profiling of Head and Neck Squamous Cell Carcinoma Tissues. Journal of Proteome Research, 2011, 10, 5232-5241.	3.7	97
220	Development of Bifunctional Stilbene Derivatives for Targeting and Modulating Metal-Amyloid-β Species. Inorganic Chemistry, 2011, 50, 10724-10734.	4.0	75
221	The amyloidogenic SEVI precursor, PAP248-286, is highly unfolded in solution despite an underlying helical tendency. Biochimica Et Biophysica Acta - Biomembranes, 2011, 1808, 1161-1169.	2.6	31
222	Structure and membrane orientation of IAPP in its natively amidated form at physiological pH in a membrane environment. Biochimica Et Biophysica Acta - Biomembranes, 2011, 1808, 2337-2342.	2.6	229
223	A partially folded structure of amyloid-beta(1–40) in an aqueous environment. Biochemical and Biophysical Research Communications, 2011, 411, 312-316.	2.1	376
224	A Two-Site Mechanism for the Inhibition of IAPP Amyloidogenesis by Zinc. Journal of Molecular Biology, 2011, 410, 294-306.	4.2	111
225	Cross-correlations between low-Î ³ nuclei in solids via a common dipolar bath. Journal of Magnetic Resonance, 2011, 212, 95-101.	2.1	16
226	Polymorphs and Hydrates of Acyclovir. Journal of Pharmaceutical Sciences, 2011, 100, 949-963.	3.3	64
227	Innentitelbild: Inhibition of Amyloid Peptide Fibrillation by Inorganic Nanoparticles: Functional Similarities with Proteins (Angew. Chem. 22/2011). Angewandte Chemie, 2011, 123, 5096-5096.	2.0	2
228	Inhibition of Amyloid Peptide Fibrillation by Inorganic Nanoparticles: Functional Similarities with Proteins. Angewandte Chemie - International Edition, 2011, 50, 5110-5115.	13.8	248
229	Inside Cover: Inhibition of Amyloid Peptide Fibrillation by Inorganic Nanoparticles: Functional Similarities with Proteins (Angew. Chem. Int. Ed. 22/2011). Angewandte Chemie - International Edition, 2011, 50, 4992-4992.	13.8	4
230	Absorbance-based assay for membrane disruption by antimicrobial peptides and synthetic copolymers using pyrroloquinoline quinone-loaded liposomes. Analytical Biochemistry, 2011, 411, 194-199.	2.4	4
231	Nanoparticle Processing of Cholesterol-Lowering Drug. , 2011, , 263-283.		0
232	Chemical shift tensor – The heart of NMR: Insights into biological aspects of proteins. Progress in Nuclear Magnetic Resonance Spectroscopy, 2010, 57, 181-228.	7.5	166
233	NMR Structure of Pardaxin, a Pore-forming Antimicrobial Peptide, in Lipopolysaccharide Micelles. Journal of Biological Chemistry, 2010, 285, 3883-3895.	3.4	123
234	Antimicrobial and Membrane Disrupting Activities of a Peptide Derived from the Human Cathelicidin Antimicrobial Peptide LL37. Biophysical Journal, 2010, 98, 248-257.	0.5	121

#	Article	IF	CITATIONS
235	Amphipathic Helical Cationic Antimicrobial Peptides Promote Rapid Formation of Crystalline States in the Presence of Phosphatidylglycerol: Lipid Clustering in Anionic Membranes. Biophysical Journal, 2010, 98, 2564-2573.	0.5	56
236	Structure, Interactions, and Antibacterial Activities of MSI-594 Derived Mutant Peptide MSI-594F5A in Lipopolysaccharide Micelles: Role of the Helical Hairpin Conformation in Outer-Membrane Permeabilization. Journal of the American Chemical Society, 2010, 132, 18417-18428.	13.7	104
237	Proton-Evolved Local-Field Solid-State NMR Studies of Cytochrome <i>b</i> ₅ Embedded in Bicelles, Revealing both Structural and Dynamical Information. Journal of the American Chemical Society, 2010, 132, 5779-5788.	13.7	35
238	Use of a Copper-Chelated Lipid Speeds Up NMR Measurements from Membrane Proteins. Journal of the American Chemical Society, 2010, 132, 6929-6931.	13.7	69
239	Homogeneous Nanoparticles To Enhance the Efficiency of a Hydrophobic Drug, Antihyperlipidemic Probucol, Characterized by Solid-State NMR. Molecular Pharmaceutics, 2010, 7, 299-305.	4.6	38
240	Probing the Spontaneous Membrane Insertion of a Tail-Anchored Membrane Protein by Sum Frequency Generation Spectroscopy. Journal of the American Chemical Society, 2010, 132, 15112-15115.	13.7	57
241	Natural-Abundance ⁴³ Ca Solid-State NMR Spectroscopy of Bone. Journal of the American Chemical Society, 2010, 132, 11504-11509.	13.7	67
242	Role of Zinc in Human Islet Amyloid Polypeptide Aggregation. Journal of the American Chemical Society, 2010, 132, 8973-8983.	13.7	212
243	INEPT-Based Separated-Local-Field NMR Spectroscopy: A Unique Approach To Elucidate Side-Chain Dynamics of Membrane-Associated Proteins. Journal of the American Chemical Society, 2010, 132, 9944-9947.	13.7	24
244	Cholesterol reduces pardaxin's dynamics—a barrel-stave mechanism of membrane disruption investigated by solid-state NMR. Biochimica Et Biophysica Acta - Biomembranes, 2010, 1798, 223-227.	2.6	88
245	Special issue on "Membrane Protein Dynamics: Correlating Structure to Functionâ€: Biochimica Et Biophysica Acta - Biomembranes, 2010, 1798, 65-67.	2.6	2
246	Probing the "Charge Cluster Mechanism―in Amphipathic Helical Cationic Antimicrobial Peptides. Biochemistry, 2010, 49, 4076-4084.	2.5	141
247	Limiting an Antimicrobial Peptide to the Lipidâ^'Water Interface Enhances Its Bacterial Membrane Selectivity: A Case Study of MSI-367. Biochemistry, 2010, 49, 10595-10605.	2.5	64
248	Design of small molecules that target metal-AÎ ² species and regulate metal-induced AÎ ² aggregation and neurotoxicity. Proceedings of the National Academy of Sciences of the United States of America, 2010, 107, 21990-21995.	7.1	253
249	Solid-State NMR Reveals the Hydrophobic-Core Location of Poly(amidoamine) Dendrimers in Biomembranes. Journal of the American Chemical Society, 2010, 132, 8087-8097.	13.7	95
250	Helical Hairpin Structure of a Potent Antimicrobial Peptide MSIâ€594 in Lipopolysaccharide Micelles by NMR Spectroscopy. Chemistry - A European Journal, 2009, 15, 2036-2040.	3.3	89
251	Multifunctional host defense peptides: functional and mechanistic insights from NMR structures of potent antimicrobial peptides. FEBS Journal, 2009, 276, 6465-6473.	4.7	88
252	Beyond NMR spectra of antimicrobial peptides: Dynamical images at atomic resolution and functional insights. Solid State Nuclear Magnetic Resonance, 2009, 35, 201-207.	2.3	139

#	Article	IF	CITATIONS
253	Efficient cross-polarization using a composite 0° pulse for NMR studies on static solids. Journal of Magnetic Resonance, 2009, 196, 105-109.	2.1	20
254	Determining the Effects of Lipophilic Drugs on Membrane Structure by Solid-State NMR Spectroscopy: The Case of the Antioxidant Curcumin. Journal of the American Chemical Society, 2009, 131, 4490-4498.	13.7	245
255	Fluorine—a new element in the design of membrane-active peptides. Molecular BioSystems, 2009, 5, 1143.	2.9	60
256	Nanoparticle Processing in the Solid State Dramatically Increases the Cell Membrane Permeation of a Cholesterol-Lowering Drug, Probucol. Molecular Pharmaceutics, 2009, 6, 1029-1035.	4.6	26
257	Association of Highly Compact Type II Diabetes Related Islet Amyloid Polypeptide Intermediate Species at Physiological Temperature Revealed by Diffusion NMR Spectroscopy. Journal of the American Chemical Society, 2009, 131, 7079-7085.	13.7	143
258	NMR Structure in a Membrane Environment Reveals Putative Amyloidogenic Regions of the SEVI Precursor Peptide PAP _{248â^'286} . Journal of the American Chemical Society, 2009, 131, 17972-17979.	13.7	62
259	Induction of Negative Curvature as a Mechanism of Cell Toxicity by Amyloidogenic Peptides: The Case of Islet Amyloid Polypeptide. Journal of the American Chemical Society, 2009, 131, 4470-4478.	13.7	130
260	Small Molecule Modulators of Copper-Induced Al ² Aggregation. Journal of the American Chemical Society, 2009, 131, 16663-16665.	13.7	189
261	Structure, membrane orientation, mechanism, and function of pexiganan — A highly potent antimicrobial peptide designed from magainin. Biochimica Et Biophysica Acta - Biomembranes, 2009, 1788, 1680-1686.	2.6	279
262	Solid-state NMR and molecular dynamics simulations reveal the oligomeric ion-channels of TM2-GABAA stabilized by intermolecular hydrogen bonding. Biochimica Et Biophysica Acta - Biomembranes, 2009, 1788, 686-695.	2.6	41
263	High-resolution Structures of Membrane-Bound IAPP Reveal Functional Implications of the Toxicity of Prefibrillar States of Amyloidogenic Proteins. Biophysical Journal, 2009, 96, 92a-93a.	0.5	0
264	An α-Helical Conformation of the SEVI Peptide, a Dramatic Enhancer of HIV Infectivity, Promotes Lipid Aggregation and Fusion. Biophysical Journal, 2009, 96, 93a-94a.	0.5	0
265	Helical Conformation of the SEVI Precursor Peptide PAP248-286, a Dramatic Enhancer of HIV Infectivity, Promotes Lipid Aggregation and Fusion. Biophysical Journal, 2009, 97, 2474-2483.	0.5	43
266	Three-Dimensional Structure and Orientation of Rat Islet Amyloid Polypeptide Protein in a Membrane Environment by Solution NMR Spectroscopy. Journal of the American Chemical Society, 2009, 131, 8252-8261.	13.7	142
267	Comprehensive Analysis of Lipid Dynamics Variation with Lipid Composition and Hydration of Bicelles Using Nuclear Magnetic Resonance (NMR) Spectroscopy. Langmuir, 2009, 25, 7010-7018.	3.5	48
268	Chemical Structure Effects on Bone Response to Mechanical Loading. Biophysical Journal, 2009, 96, 409a.	0.5	0
269	Time-Resolved Dehydration-Induced Structural Changes in an Intact Bovine Cortical Bone Revealed by Solid-State NMR Spectroscopy. Journal of the American Chemical Society, 2009, 131, 17064-17065.	13.7	104
270	Quantum dots as mineral- and matrix-specific strain gages for bone biomechanical studies. Proceedings of SPIE, 2009, , .	0.8	1

#	Article	IF	CITATIONS
271	Bicelles – A Much Needed Magic Wand to Study Membrane Proteins by NMR Spectroscopy. , 2009, , 117-128.		3
272	Using Fluorous Amino Acids to Modulate the Biological Activity of an Antimicrobial Peptide. ChemBioChem, 2008, 9, 370-373.	2.6	109
273	Bicelleâ€Enabled Structural Studies on a Membraneâ€Associated Cytochromeâ€b ₅ by Solidâ€State MAS NMR Spectroscopy. Angewandte Chemie - International Edition, 2008, 47, 7864-7867.	² 13.8	51
274	NMR Structure of the Cathelicidin-Derived Human Antimicrobial Peptide LL-37 in Dodecylphosphocholine Micelles. Biochemistry, 2008, 47, 5565-5572.	2.5	157
275	Freezing Point Depression of Water in Phospholipid Membranes: A Solid-State NMR Study. Langmuir, 2008, 24, 13598-13604.	3.5	28
276	Amyloid Fiber Formation and Membrane Disruption are Separate Processes Localized in Two Distinct Regions of IAPP, the Type-2-Diabetes-Related Peptide. Journal of the American Chemical Society, 2008, 130, 6424-6429.	13.7	214
277	Studies on anticancer activities of antimicrobial peptides. Biochimica Et Biophysica Acta - Biomembranes, 2008, 1778, 357-375.	2.6	1,036
278	Using Fluorous Amino Acids To Probe the Effects of Changing Hydrophobicity on the Physical and Biological Properties of the β-Hairpin Antimicrobial Peptide Protegrin-1. Biochemistry, 2008, 47, 9243-9250.	2.5	80
279	Nitrogen-14 Solid-State NMR Spectroscopy of Aligned Phospholipid Bilayers to Probe Peptideâ^'Lipid Interaction and Oligomerization of Membrane Associated Peptides. Journal of the American Chemical Society, 2008, 130, 11023-11029.	13.7	46
280	High-Resolution Characterization of Liquid-Crystalline [60]Fullerenes Using Solid-State Nuclear Magnetic Resonance Spectroscopy. Journal of Physical Chemistry B, 2008, 112, 12347-12353.	2.6	19
281	A Single Mutation in the Nonamyloidogenic Region of Islet Amyloid Polypeptide Greatly Reduces Toxicity. Biochemistry, 2008, 47, 12680-12688.	2.5	142
282	Structures of Rat and Human Islet Amyloid Polypeptide IAPP _{1â^'19} in Micelles by NMR Spectroscopy. Biochemistry, 2008, 47, 12689-12697.	2.5	161
283	Two-dimensional homonuclear chemical shift correlation established by the cross-relaxation driven spin diffusion in solids. Journal of Chemical Physics, 2008, 128, 052308.	3.0	30
284	Membrane fragmentation by an amyloidogenic fragment of human Islet Amyloid Polypeptide detected by solid-state NMR spectroscopy of membrane nanotubes. Biochimica Et Biophysica Acta - Biomembranes, 2007, 1768, 2026-2029.	2.6	131
285	The cytochromes P450 and b5 and their reductases—Promising targets for structural studies by advanced solid-state NMR spectroscopy. Biochimica Et Biophysica Acta - Biomembranes, 2007, 1768, 3235-3259.	2.6	107
286	NMR structural studies on membrane proteins. Biochimica Et Biophysica Acta - Biomembranes, 2007, 1768, 2947-2948.	2.6	6
287	Ultrastrong and Stiff Layered Polymer Nanocomposites. Science, 2007, 318, 80-83.	12.6	1,500
288	Solid-State NMR Reveals Structural and Dynamical Properties of a Membrane-Anchored Electron-Carrier Protein, Cytochromeb5. Journal of the American Chemical Society, 2007, 129, 6670-6671.	13.7	121

#	Article	IF	CITATIONS
289	Structure, Topology, and Tilt of Cell-Signaling Peptides Containing Nuclear Localization Sequences in Membrane Bilayers Determined by Solid-State NMR and Molecular Dynamics Simulation Studies. Biochemistry, 2007, 46, 965-975.	2.5	63
290	High-Resolution 2D NMR Spectroscopy of Bicelles To Measure the Membrane Interaction of Ligands. Journal of the American Chemical Society, 2007, 129, 794-802.	13.7	62
291	Sensitivity and resolution enhancement in solid-state NMR spectroscopy of bicelles. Journal of Magnetic Resonance, 2007, 184, 228-235.	2.1	45
292	Atomistic-Resolution Structural Studies of Liquid Crystalline Materials Using Solid-State NMR Techniques. , 2007, , 85-116.		5
293	Structures of the Dimeric and Monomeric Variants of Magainin Antimicrobial Peptides (MSI-78 and) Tj ETQq1 1 C).784314 r 2.5	gBŢ <i>¦</i> Overloc
294	Deletion of All Cysteines in Tachyplesin I Abolishes Hemolytic Activity and Retains Antimicrobial Activity and Lipopolysaccharide Selective Binding. Biochemistry, 2006, 45, 6529-6540.	2.5	109
295	Solid-State NMR Investigation of the Membrane-Disrupting Mechanism of Antimicrobial Peptides MSI-78 and MSI-594 Derived from Magainin 2 and Melittin. Biophysical Journal, 2006, 91, 206-216.	0.5	246
296	A High-Resolution Solid-State NMR Approach for the Structural Studies of Bicelles. Journal of the American Chemical Society, 2006, 128, 6326-6327.	13.7	60
297	The spectrum of antimicrobial activity of the bacteriocin subtilosin A. Journal of Antimicrobial Chemotherapy, 2006, 59, 297-300.	3.0	166
298	Cell selectivity correlates with membrane-specific interactions: A case study on the antimicrobial peptide G15 derived from granulysin. Biochimica Et Biophysica Acta - Biomembranes, 2006, 1758, 154-163.	2.6	63
299	LL-37, the only human member of the cathelicidin family of antimicrobial peptides. Biochimica Et Biophysica Acta - Biomembranes, 2006, 1758, 1408-1425.	2.6	822
300	The human beta-defensin-3, an antibacterial peptide with multiple biological functions. Biochimica Et Biophysica Acta - Biomembranes, 2006, 1758, 1499-1512.	2.6	269
301	Separated local field NMR spectroscopy by windowless isotropic mixing. Chemical Physics Letters, 2006, 419, 168-173.	2.6	19
302	Measurement of heteronuclear dipolar couplings using a rotating frame solid-state NMR experiment. Chemical Physics Letters, 2006, 419, 533-536.	2.6	30
303	Heteronuclear isotropic mixing separated local field NMR spectroscopy. Journal of Chemical Physics, 2006, 125, 034507.	3.0	61
304	How Far Can the Sensitivity of NMR Be Increased?. Annual Reports on NMR Spectroscopy, 2006, 58, 155-175.	1.5	44
305	Membrane permeabilization, orientation, and antimicrobial mechanism of subtilosin A. Chemistry and Physics of Lipids, 2005, 137, 38-51.	3.2	109
306	Broadband-PISEMA solid-state NMR spectroscopy. Chemical Physics Letters, 2005, 407, 289-293.	2.6	54

#	Article	IF	CITATIONS
307	PITANSEMA-MAS, a solid-state NMR method to measure heteronuclear dipolar couplings under MAS. Chemical Physics Letters, 2005, 408, 118-122.	2.6	28
308	Solution Structure and Interaction of the Antimicrobial Polyphemusins with Lipid Membranesâ€,‡. Biochemistry, 2005, 44, 15504-15513.	2.5	100
309	Solid-State NMR Characterization and Determination of the Orientational Order of a Nematogen. Journal of Physical Chemistry B, 2005, 109, 19696-19703.	2.6	27
310	Solid-State NMR Characterization of a Novel Thiophene-Based Three Phenyl Ring Mesogen. Chemistry of Materials, 2005, 17, 4567-4569.	6.7	25
311	A 2D Solid-State NMR Experiment To Resolve Overlapping Aromatic Resonances of Thiophene-Based Nematogens. Journal of the American Chemical Society, 2005, 127, 6958-6959.	13.7	36
312	Synthetic and Natural Polycationic Polymer Nanoparticles Interact Selectively with Fluid-Phase Domains of DMPC Lipid Bilayers. Langmuir, 2005, 21, 8588-8590.	3.5	128
313	Antimicrobial activity and membrane selective interactions of a synthetic lipopeptide MSI-843. Biochimica Et Biophysica Acta - Biomembranes, 2005, 1711, 49-58.	2.6	106
314	Membrane Thinning Due to Antimicrobial Peptide Binding: An Atomic Force Microscopy Study of MSI-78 in Lipid Bilayers. Biophysical Journal, 2005, 89, 4043-4050.	0.5	194
315	Synthesis and 13C CPMAS NMR Characterization of Novel Thiophene-Based Nematogens. Chemistry of Materials, 2005, 17, 2013-2018.	6.7	40
316	PISEMA Solid-State NMR Spectroscopy. Annual Reports on NMR Spectroscopy, 2004, 52, 1-52.	1.5	165
317	Structure and Orientation of Pardaxin Determined by NMR Experiments in Model Membranes. Journal of Biological Chemistry, 2004, 279, 45815-45823.	3.4	157
318	A study of a Cα,β-didehydroalanine homo-oligopeptide series in the solid-state by13C cross-polarization magic angle spinning NMR. Journal of Peptide Science, 2004, 10, 336-341.	1.4	9
319	Effects of antidepressants on the conformation of phospholipid headgroups studied by solid-state NMR. Magnetic Resonance in Chemistry, 2004, 42, 105-114.	1.9	60
320	Guest Editors' Foreword: Solid-state NMR on biological systems. Magnetic Resonance in Chemistry, 2004, 42, 86-86.	1.9	1
321	Direct observation of lipid bilayer disruption by poly(amidoamine) dendrimers. Chemistry and Physics of Lipids, 2004, 132, 3-14.	3.2	221
322	Investigation of the interaction of myelin basic protein with phospholipid bilayers using solid-state NMR spectroscopy. Chemistry and Physics of Lipids, 2004, 132, 47-54.	3.2	18
323	PITANSEMA, a low-power PISEMA solid-state NMR experiment. Chemical Physics Letters, 2004, 399, 359-362.	2.6	36
324	How Does an Amide-15N Chemical Shift Tensor Vary in Peptides?. Journal of Physical Chemistry B, 2004, 108, 16577-16585.	2.6	54

#	Article	IF	CITATIONS
325	Solid-State NMR Spectroscopy of Aligned Lipid Bilayers at Low Temperatures. Journal of the American Chemical Society, 2004, 126, 2318-2319.	13.7	17
326	Ab Initio Study of13CαChemical Shift Anisotropy Tensors in Peptides. Journal of the American Chemical Society, 2004, 126, 8529-8534.	13.7	44
327	Conformational preferences of the amylin nucleation site in SDS micelles: An NMR study. Biopolymers, 2003, 69, 29-41.	2.4	60
328	Determination of the conformation and stability of simple homopolypeptides using solid-state NMR. Solid State Nuclear Magnetic Resonance, 2003, 24, 94-109.	2.3	34
329	Interaction of Cd and Zn with Biologically Important Ligands Characterized Using Solid-State NMR and ab Initio Calculations. Inorganic Chemistry, 2003, 42, 3142-3151.	4.0	42
330	Characterization of Metal Centers in Bioinorganic Complexes Using Ab Initio Calculations of113Cd Chemical Shifts. Inorganic Chemistry, 2003, 42, 2200-2202.	4.0	16
331	Nuclear magnetic resonance studies of metals in solid state non-metallic materials. Materials Science and Technology, 2003, 19, 1191-1196.	1.6	6
332	Quantum Chemical Calculations of Cadmium Chemical Shifts in Inorganic Complexes. Journal of Physical Chemistry A, 2002, 106, 10363-10369.	2.5	22
333	An Innovative Procedure Using a Sublimable Solid to Align Lipid Bilayers for Solid-State NMR Studies. Biophysical Journal, 2002, 82, 2499-2503.	0.5	99
334	One-dimensional 1H-detected solid-state NMR experiment to determine amide-1H chemical shifts in peptides. Chemical Physics Letters, 2002, 351, 42-46.	2.6	16
335	Solid-State13C NMR Chemical Shift Anisotropy Tensors of Polypeptides. Journal of the American Chemical Society, 2001, 123, 6118-6126.	13.7	122
336	An Experimental Strategy to Dramatically Reduce the RF Power Used in Cross Polarization Solid-State NMR Spectroscopy. Journal of the American Chemical Society, 2001, 123, 7467-7468.	13.7	26
337	Orientation of Amide-Nitrogen-15 Chemical Shift Tensors in Peptides:Â A Quantum Chemical Study. Journal of the American Chemical Society, 2001, 123, 914-922.	13.7	91
338	A Two-Dimensional Magic-Angle Decoupling and Magic-Angle Turning Solid-State NMR Method:Â An Application to Study Chemical Shift Tensors from Peptides That Are Nonselectively Labeled with15N Isotope. Journal of Physical Chemistry B, 2001, 105, 4752-4762.	2.6	33
339	The unitary evolution operator for cross-polarization schemes in NMR. Chemical Physics Letters, 2001, 342, 127-134.	2.6	21
340	2D – isotropic chemical shift correlation established by – dipolar coherence transfer in biological solids. Chemical Physics Letters, 2001, 342, 312-316.	2.6	22
341	Characterization of 15N Chemical Shift and 1Hâ^15N Dipolar Coupling Interactions in a Peptide Bond of Uniaxially Oriented and Polycrystalline Samples by One-Dimensional Dipolar Chemical Shift Solid-State NMR Spectroscopy. Journal of the American Chemical Society, 1998, 120, 8868-8874.	13.7	62
342	Complete resolution of the solid-state NMR spectrum of a uniformly 15N-labeled membrane protein in phospholipid bilayers. Proceedings of the National Academy of Sciences of the United States of America, 1997, 94, 8551-8556.	7.1	209

#	Article	IF	CITATIONS
343	Magnitudes and Orientations of the Principal Elements of the1H Chemical Shift,1Hâ [~] 15N Dipolar Coupling, and15N Chemical Shift Interaction Tensors in15Nε1-Tryptophan and15Nπ-Histidine Side Chains Determined by Three-Dimensional Solid-State NMR Spectroscopy of Polycrystalline Samples. Journal of the American Chemical Society, 1997, 119, 10479-10486.	13.7	70
344	Three-Dimensional Solid-State NMR Experiment That Correlates the Chemical Shift and Dipolar Coupling Frequencies of Two Heteronuclei. Journal of Magnetic Resonance Series B, 1995, 107, 88-90.	1.6	76
345	Four-Dimensional Solid-State NMR Experiment That Correlates the Chemical-Shift and Dipolar-Coupling Frequencies of Two Heteronuclei with the Exchange of Dilute-Spin Magnetization. Journal of Magnetic Resonance Series B, 1995, 109, 112-116.	1.6	38
346	Three-dimensional solid-state NMR spectroscopy of a peptide oriented in membrane bilayers. Journal of Biomolecular NMR, 1995, 6, 329-34.	2.8	80
347	Two-dimensional chemical shift/heteronuclear dipolar coupling spectra obtained with polarization inversion spin exchange at the magic angle and magic-angle sample spinning (PISEMAMAS). Solid State Nuclear Magnetic Resonance, 1995, 4, 387-392.	2.3	80
348	High-Resolution Heteronuclear Dipolar Solid-State NMR Spectroscopy. Journal of Magnetic Resonance Series A, 1994, 109, 270-272.	1.6	403
349	Analysis of the Performance of NQR Composite Pulses. Journal of Magnetic Resonance Series A, 1993, 102, 274-286.	1.6	15
350	An RF Pulse Sequence Optimized for Homonuclear J Cross Polarization under Magic-Angle-Spinning Conditions in Solids. Journal of Magnetic Resonance Series A, 1993, 104, 366-368.	1.6	10
351	Dipolar HOHAHA under MAS conditions for solid-state NMR. Chemical Physics Letters, 1993, 212, 81-84.	2.6	59
352	Broadband excitation sequences for NQR spectroscopy. Molecular Physics, 1991, 73, 207-219.	1.7	10
353	Double quantum nuclear quadrupole resonance spectroscopy of spinl= 7/2 nuclei in zero magnetic field. Molecular Physics, 1991, 72, 1425-1429.	1.7	7
354	Generalized theory of multiple-pulse zero-time resolution in spin-32 NQR spectroscopy. Chemical Physics Letters, 1990, 168, 401-404.	2.6	4
355	Design of composite pulses for nuclear quadrupole resonance spectroscopy. Journal of Molecular Structure, 1989, 192, 333-344.	3.6	16